Sustainable Energy Technologies and Assessments 40 (2020) 100754

Contents lists available at ScienceDirect

Sustainable Energy Technologies and Assessments

journal homepage: www.elsevier.com/locate/seta

Contribution for bidding of wind-photovoltaic on grid farms based on NBI-EFA-SNR method

Giancarlo Aquila[a], Anderson Rodrigo de Queiroz[b], Paulo Rotela Junior[c,*], Luiz Célio Souza Rocha[d], Edson de Oliveira Pamplona[e], Pedro Paulo Balestrassi[e]

[a] Institute of Electrical and Energy Systems, Federal University of Itajubá, Itajubá MG, Brazil
[b] School of Business, North Carolina Central University, Raleigh-Durham, NC, United States
[c] Department of Production Engineering, Federal University of Paraiba, Joao Pessoa, PB, Brazil
[d] Federal Institute of Education, Science and Technology, North of Minas Gerais, Almenara, MG, Brazil
[e] Institute of Production Engineering and Management, Federal University of Itajuba, Itajuba, MG, Brazil

ARTICLE INFO

Keywords:
Hybrid System
Non-Linear Optimization
Energy Planning
Sustainable Energy
Electricity Production

ABSTRACT

Methods for supporting the bidding processes of hybrid wind-photovoltaic (W-PV) farms are scarce, especially when numerous goals are included in the optimization problem. Therefore, the primary objective of this study is to develop a novel model that can help bidding of W-PV farms considering a range of objectives that maximize the environmental and welfare benefits. This new approach contributes to energy planning for any type of hybrid farm through multi-objective programming, even in cases where the optimization of several correlated outputs is desired. Using the proposed approach the optimal system configuration can be obtained in these cases with low computational costs. A non-linear multi-objective optimization (NL-MO) is proposed to optimize the area occupied by the W-PV farm, minimum feasibility price, electricity production expected, and standard-deviation of the electricity produced. The model has been elaborated from non-linear optimization using the normal-boundary intersection (NBI) method, exploratory factor analysis (EFA), and Taguchi signal-to-noise ratio (SNR). The optimal values for the response variables are an area of 132.92 km^2, minimum price of 182.95 R$/MWh, annual electricity production of 72.17 GWh, with a standard deviation of 1.74 GWh and the ideal share is 41% wind power and 59% PV power.

Introduction

Currently as the demand for energy has been growing rapidly worldwide, one of the great challenges is energy security [1–3]. The energy market must meet this rising energy demand, which goes beyond limiting fossil fuel reserves [4]. Increasing populations, instable access to energy sources, economic and urban growth, and water scarcity, especially in desert and arid regions, are among the key obstacles [5].

In this scenario, renewable energy technologies (RET) can contribute to the supply of electricity with low greenhouse gas (GHG) emissions [6–8]. To promote the growth of RETs, governments in several countries have resorted to policy schemes, such as feed-in tariffs, quotas with trading green certificates (TGC), and energy auctions [5,9]. The renewable energy source (RES) policy schemes encourage the development of the RES market by attracting the capital of investors primarily by increasing the user network. As this network grows, it generates learning gains (spillovers), favoring the reduction in the technological cost for the production of green electricity through RESs [10–12].

Other benefits promoted by the RES policy schemes are improved energy efficiency in the production process and the increase in the ratio

Abbreviations: W-PV, wind-photovoltaic; NL-MO, non-linear multi-objective optimization; NBI, normal-boundary intersection; EFA, exploratory factor analysis; SNR, signal-to-noise ratio; RET, renewable energy technologies; GHG, greenhouse gas; TGC, trading green certificates; RES, renewable energy source; TOPSIS, technique for order preference by similarity to ideal solution; LCOE, levelized cost of electricity; AEP, average electricity production; sdAEP, standard deviation of the AEP; Pmin, minimum price; MDOE, mixture design of experiment; MCS, Monte Carlo simulation; AWEP, annual wind electricity production; APVEP, the annual PV electricity production; SWERA, solar and wind energy resource assesment; APVEP, average PV electricity production; NPV, net present value; WACC, weighted average capital cost; CAPM, capital asset pricing model

* Corresponding author at: BPS, Av., 1303, Itajuba, MG 37500-015, Brazil.
E-mail addresses: giancarlo.aquila@yahoo.com (G. Aquila), ar_queiroz@yahoo.com (A.R. de Queiroz), paulo.rotela@gmail.com (P. Rotela Junior), luizrochamg@hotmail.com (L.C.S. Rocha), pamplona@unifei.edu.br (E.d.O. Pamplona), ppbalestrassi@gmail.com (P.P. Balestrassi).

https://doi.org/10.1016/j.seta.2020.100754
Received 13 March 2020; Received in revised form 25 May 2020; Accepted 27 May 2020

of electric energy to the total primary energy, with a significant portion coming from green electricity [13]. Consequently, the share of RETs in electricity generation has increased, making energy planning more complex.

The entry of intermittent sources, such as wind and PV, in the electricity matrices increases the relevance of improving aspects that go beyond decreasing generation costs, such as energy security, reliability, flexibility, and the reduction in GHG emissions [14]. Multi-objective optimization methods are a way to support these complex energy planning decisions.

Previous studies by Park et al. [15], Kannan et al. [16], and Sirikum et al. [17] used formulations that included only cost minimization as the primary objective. However, with these models, the optimal function is reached without considering conflicting objectives. In energy planning, classical models that include cost minimization as the only objective have become unrealistic as more attributes are required [14]. Multi-objective optimization methods have been used as a solution for similar problems with more than one objective. Certain previous studies presented in the literature have used multi-objective optimization for the planning of hybrid systems.

Mavrotas et al. [18] formulated a multi-objective model for planning the electrical system in Greece based on the branch-and-bound technique to generate and compare a set of efficient solutions for the pair. This model aimed to reduce the cost and carbon emissions, and the study addressed a series of technical restrictions of the system. Afterwards, Antunes et al. [19] presented a multi-objective linear programming model for planning the expansion of electricity generation with the objective of minimizing the total cost of expansion and its environmental impacts.

Aghaei et al. [20] proposed a multi-objective model for planning a system with the purpose of minimizing costs, environmental impacts, energy consumption from fossil fuels, and the exposure to volatility in the import price of fossil fuels and increasing the reliability of the system. The problem was formulated using mixed integer linear programming and solved using the ε-method. Vahidinasab and Jadid [21] formulated a model using the normal-boundary intersection (NBI) focusing on the strategy of contracting electric-generation projects, minimizing the power flow combined with coefficients that represent the emission of pollutants and maximizing production, including physical generation restrictions.

Aghaei et al. [22] developed a multi-objective programming based on the NBI, aiming at generation expansion that prioritizes minimizing costs and environmental impacts, in addition to maximizing reliability.

Ahmadi et al. [23] used multi-objective programming through the NBI to integrate thermal plants with high voltage networks to minimize costs and GHG emissions. An approach called the technique for order preference by similarity to ideal solution (TOPSIS) was used to determine the best Pareto-optimal solution.

Izadbakhsh et al. [24] developed an optimization model to determine the best mix of micro wind turbines, photovoltaic panels, fuel oil generators, battery banks, and larger wind turbines for a small off-grid generation system. The NBI method was used with two objective functions: one to minimize the total cost of the system and the other to minimize pollutant emissions. TOPSIS fuzzy was used to choose the best Pareto-optimal solution.

Luz et al. [25] addressed solutions for the expansion of the Brazilian electrical system through different techniques of multi-objective linear programming. The models were based on the new government targets for RESs, considering three objective functions: minimizing the total cost and maximizing the peak load generation and the contribution of non-hydro RESs.

Fonseca et al. [26] proposed an optimization model to determine the best combination for a diesel-PV off-grid system in the Amazon region. The results were then compared with those found using the Homer® software. The authors performed the NBI method for nonlinear multi-objective optimization (NL-MO), considering the minimization of GHG emissions and the levelized cost of electricity (LCOE). The model aimed to guide investors regarding isolated diesel-PV generation systems and used data envelopment analysis as an ex-post method to obtain the best Pareto-optimal solution.

Roberts et al. [27] presented an NL-MO simulation-based approach to dimension an off-grid hybrid generation system based on diesel and RES. This method integrates a genetic algorithm model and a simulation module to represent the operation of an isolated hybrid system. The objectives considered are the uncertainties related to RES availability, level of demand, and likelihood of equipment failure. The performance of the model was evaluated using actual conditions for an off-grid system in rural communities in the Amazon region.

Aquila et al. [28] developed an NL-MO method to help Brazilian electricity regulators to contract W-PV farms on grid considering economic and environmental aspects. However, the developed method was computationally complex and not appropriate for decisions requiring numerous, possibly correlated, objectives to determine the optimal parameters of a W-PV farm.

We can observe that the literature about energy planning supported by NL-MO methods usually investigates electricity systems expansion or off-grid systems planning. Although studies related to the planning of hybrid W-PV farms on grid are still incipient, for both regulators and investors is relevant NL-MO methods focused on define share of W-PV farms based on criteria that optimize relevant objectives for stakeholders. Thus, it becomes possible to feasible W-PV bidding process, since the developed model allows to standardize the process of defining share of each source for W-PV farms that will compete in the bidding.

Thus, the present study aims to develop and validate a proposal that fills the gaps presented in Aquila et al. [28]. Furthermore, the proposed model is not specifically geared to serve only the Brazilian electricity system but is also applicable to other types of electrical systems with low computational costs. Another novelty of the study is the application of multivariate statistical analysis to improve the NL-MO process of bidding for W-PV farms by managing correlated responses.

In a practical approach, the NBI-EFA-SNR method proposed in this study can help the regulator to impose a standard for the competitors of a bidding process for W-PV farms to configure the shares of the projects. Initially, bidders must plan the W-PV farm using the standard method and so they would be able to compete isn the bidding. Thereby, a bidding process between W-PV farms configured using the same criteria would become viable.

Since hybrid W-PV farms optimization can involve several correlated outputs, the proposed methodology allows to reduce the computational cost without neglecting any output. Thus, the objective of this study will present the following logical sequence: the need to define parameters for contracting W-PV farms; presence of several outputs to be considered, of an economic, social and technical aspects; existence of a large number of correlated characteristics; use of multivariate analysis methods to reduce the problem, without neglecting any information; share definition of each source in the W-PV farms, serving as a basis for policy-makers during the hiring process.

Although the case study in this paper is based on a farm located in Brazil, the proposal may also be adapted and applied to W-PV farms in other localities. The analyzed outputs are the average electricity production (AEP), standard deviation of the AEP (*sd*AEP), ideal occupied area, and minimum price (P_{min}) that allows for financial viability of the W-PV farm.

Materials and methods

This section describes the main tools explored in the development of the method, including NL-MO from NBI, exploratory factor analysis (EFA), Taguchi signal-to-noise ratio (SNR), and mixture design of experiment (MDOE).

In practical situations, where the required effort or desired benefit can be expressed as a function of certain decision variables,

optimization is a procedure maximize or minimize the value of a function [29]. In an optimization problem, the first step is recognizing the problem objective that is represented by a quantitative measure that represents the system performance [30].

Decision variables can be restricted in certain way, for e.g., as a molecule density and an interest rate that cannot be negative. Problem of identifying variables, objectives, and constraints to describe a problem is known as modeling.

Mathematically, an optimization problem can be represented as follows:

$$\underset{x\in R^n}{Min} f(x)$$

$$subject\ to: \begin{matrix} c_i(x) = 0,\ i \in \varepsilon \\ c_i(x) \leqslant 0,\ i \in I \end{matrix} \quad (1)$$

where **x** is the vector of the decision variables, f is the objective function, c_i are the functions of constraints, and ε and I comprise the set of equality and inequality constraints.

Usually, in multi-objective optimization problems, the equations that represent the processes to be optimized are not previously known. Thus, a modeling methodology is needed to discover the mathematical relationship between the response variables and the objective functions.

Initially, in MDOE, the input variables (x_i) are characterized as mixture components, and the responses are calculated as a function of the proportions of each component [31]. Thus, for a problem involving q mixing ingredients, the sum of the fractions of each component is equal to one [31], illustrated as follows:

$$\sum_{i=1}^{q} x_i = 1,\ x_i \geqslant 0,\ (i = 1, \ldots, q) \quad (2)$$

where x_i is the i^{th} mixture ingredient.

Experimental design for mixtures is configured using a simple coordinate system. Therefore, in this context, *simplex* designs are mostly used (see more in [31]).

The optimal configuration of W-PV hybrid systems is characterized as a mixture problem because the objective is to find the ideal share of each source in the system. As shown in Fig. 1, one of the most interesting advantages of W-PV hybrid systems is the complementarity between the sources; the wind regime is more intense at night, whereas solar radiation occurs only during the day [32–34]. In addition, if the configuration of the farm considers economic and socio-environmental aspects, the impacts resulting from the disadvantages of each source can be minimized.

For example, wind power has the following disadvantages: visual pollution, noise pollution due to the sound of the wind blowing on the blades, and the possibility of migratory bird accidents, which may lead to the death of the animals [35]. Furthermore, Ramanathan [36] noticed that wind farms occupy significant area, and consequently, the implantation of wind power farms can cause alterations to the natural landscape with limitations and disturbances for the local population, especially during the construction phase of the farm. Land leasing expenses are also increased, and available space for other productive activities is reduced.

Before performing the EFA, it is important to analyze the outputs of the problem. If there are responses with conflicting optimization directions, maximization or minimization of the factors will favor some variables, Taguchi SNR normalizes individual responses to eliminate this problem. Taguchi originally uses SNR to measure the deviations of quality characteristics from target values [37].

Variability can be analyzed by choosing an appropriate SNR [37]. Thus, three SNRs are generally used:

1) "*Smaller-the-better*" (goal is to minimize a performance):

$$SNR = -10\log\left(\frac{1}{n}\sum_{i=1}^{n} y_i^2\right) \quad (3)$$

where y is the i^{th} output observed.

2) "*Bigger-the-better*" (goal is to maximize a performance):

$$SNR = -10\log\left(\frac{1}{n}\sum_{i=1}^{n} \frac{1}{y_i^2}\right) \quad (4)$$

3) "*Nominal-is-better*" (objective is to achieve a certain nominal value):

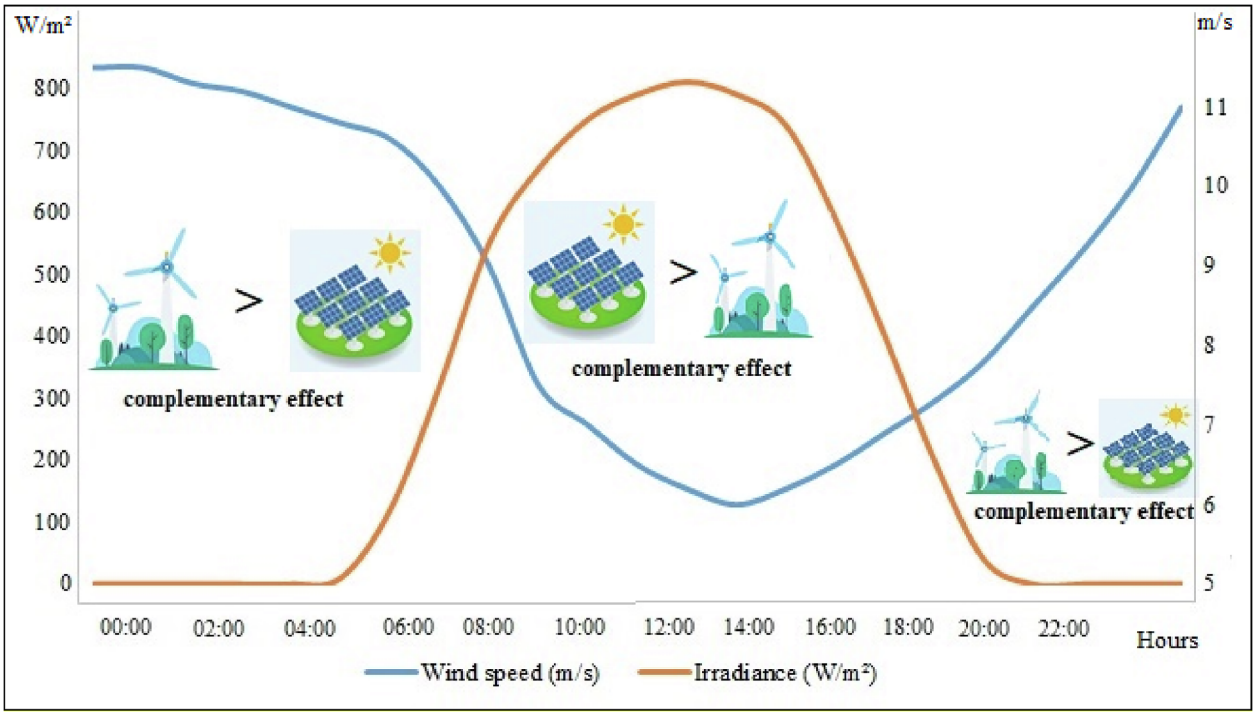

Fig. 1. Complementarity between solar irradiance and wind speed.

$$SNR = 10\log\left(\frac{\bar{y}^2}{S^2}\right) \tag{5}$$

where S is the sample standard deviation.

Thus, because the optimal levels of influence variables are those that maximize SNR [37], it is possible to standardize the optimization direction of the individual responses from SNR.

Finally, EFA attempts to explain the correlation among a set of observed variables through a linear combination of an unknown number of unobserved random factors [38]. Notably, the planner of a hybrid system could consider several outputs that may be relevant to the characteristics of the generation system. By reducing the dimensionality of the problem through EFA, the computational cost of multi-objective optimization with several outputs is also reduced.

Similarly, as a principal component analysis, EFA can reduce the dimensionality of the problem without significant loss of information through the approximation of the covariance or correlation matrix (Σ). However, EFA considers that variables can be grouped by their correlations and all variables within a particular group are highly correlated among themselves, but have small correlations with variables in other groups. Each group then represent an underlying construct or factor that is responsible for the observed correlations [39].

EFA models express each variable as a linear combination of underlying common factors ($f_1, f_2, \ldots, f_n$) with an error term ($\varepsilon_1, \varepsilon_2, \ldots, \varepsilon_n$) added which will account for the part of variable that is unique. For any $y_1, y_2, \ldots, y_n$ observation, vector y, model is as follows [40]:

$$\begin{aligned} y_1 - \mu_1 &= \lambda_{11}f_1 + \lambda_{12}f_2 + \ldots + \lambda_{1m}f_m + \varepsilon_1 \\ y_2 - \mu_2 &= \lambda_{21}f_1 + \lambda_{22}f_2 + \ldots + \lambda_{2m}f_m + \varepsilon_2 \\ &\vdots \\ y_p - \mu_p &= \lambda_{p1}f_1 + \lambda_{p2}f_2 + \ldots + \lambda_{pm}f_m + \varepsilon_p \end{aligned} \tag{6}$$

where f_m is the random variable that produces y_p, λ_{pm} is the coefficient that represents loadings and serves as a weight showing how each y_p individually depends on f_m, and $p > m$ to achieve a conservative description of the variables as functions of a few underlying factors.

Two methods can be used to estimate loadings and commonalities: the principal component (and principal factor) method, used in this study, or maximum likelihood, with a regression method to calculate the factors score (see more in [41]) [40–41]. After the factors are extracted by creating a rotation of new axes, the data is simplified allowing a better understanding of the factors [40]. In this study, we focus on methods of orthogonal rotation.

When $m = 2$, the transformation to a simple structure can be determined graphically based on a plot of factor loadings [39]. The rows of $\widehat{\Lambda}$are pairs of loadings, and the angle ϕ is that which the axes can be rotated to move them closer to a grouping of points [40]. The new rotated loadings can be calculated by $\widehat{\Lambda} * = \widehat{\Lambda}T$, where T is the sine and cosine matrix in the counterclockwise and clockwise rotation [40]:

$$T = \underbrace{\begin{bmatrix} \cos\phi & -\sin\phi \\ \sin\phi & \cos\phi \end{bmatrix}}_{counterclockwise} = \underbrace{\begin{bmatrix} \cos\phi & \sin\phi \\ -\sin\phi & \cos\phi \end{bmatrix}}_{clockwise} \tag{7}$$

The primary orthogonal rotation methods are varimax, quartimax, and equimax.

a) Varimax

Varimax is defined as a transformation with the objective of maximizing the variance, subject to constraint$\widehat{\Lambda} = \widehat{\lambda}ij$. However, this occurs only when the factor loads of column m are minimized (i.e., minimizes the complexity of factors).

$$V = \sum_{j=1}^{k}\left[\frac{1}{m}\sum_{i=1i=1}^{m}\widehat{\lambda}_{ij}^4 - \frac{1}{m^2}\left(\sum_{i=1}^{m}\widehat{\lambda}_{ij}\right)^2\right] \tag{8}$$

where$\widehat{\lambda}ij = \sum_{i=1}^{m}\widehat{\lambda}_{ij}/m$is the average of the squared loadings of factor j.

b) Quartimax

As the inverse of varimax, this method is based on the maximization of the variance of square of loadings in each line p of matrix $\widehat{\Lambda}$.

$$V = \sum_{j=1}^{k}\left[\frac{1}{p}\sum_{i=1}^{p}\widehat{\lambda}_{ij}^4 - \frac{1}{p^2}\left(\sum_{i=1}^{p}\widehat{\lambda}_{ij}\right)^2\right] \tag{9}$$

c) Equimax

Equimax considers simplifying the rows and columns of $\widehat{\Lambda}$, minimizing the complexity of the factors and variables simultaneously. Therefore, this method has been used for factor rotation in this study.

For routine optimization, NBI is an approach developed to find Pareto-optimal solutions evenly distributed for a nonlinear multi-objective problem [42]. The NBI formulation increased with the restrictions of the mixing problem, illustrated in Eq. (2), is

$$\begin{aligned} &\underset{(x,\ D)}{Max}\ D \\ s.t.:\ &\overline{\Phi}w - D\overline{\Phi}e = \overline{F}(\mathbf{x}) \\ &\sum(\mathbf{x}) = 1 \\ &\mathbf{x} \geqslant 0 \\ &\mathbf{x} \in \Omega \end{aligned} \tag{10}$$

where w is the convex weighting, D is the distance between the utopia and Pareto frontier, $\overline{F}(\mathbf{x})$ is a vector containing individual values of normalized objectives in each run, and e is a column vector of ones. Φ and $\overline{\Phi}$ are the payoff and normalized payoff matrices and can be illustrated as follows:

$$\Phi = \begin{bmatrix} f_1^*(x_1^*) & \cdots & f_1(x_m^*) \\ \vdots & \ddots & \vdots \\ f_m(x_1^*) & \cdots & f_m^*(x_m^*) \end{bmatrix} \Rightarrow \overline{\Phi} = \begin{bmatrix} \frac{f_1^*(x_1^*) - f_1^*(x_1^*)}{f_1(x_m^*) - f_1^*(x_1^*)} & \cdots & \frac{f_1(x_m^*) - f_1^*(x_1^*)}{f_m(x_m^*) - f_1^*(x_1^*)} \\ \vdots & \ddots & \vdots \\ \frac{f_m(x_1^*) - f_m^*(x_m^*)}{f_m(x_1^*) - f_m^*(x_m^*)} & \cdots & \frac{f_m^*(x_m^*) - f_m^*(x_m^*)}{f_m(x_1^*) - f_m^*(x_m^*)} \end{bmatrix} \tag{11}$$

where $f_i^*(x_i^*)$ is the solution that minimizes the i-th objective function $f_i(x)$; $f_i(x_i^*)$ is the remaining objective function when $f_i^*(x_i^*)$ is optimized.

The ex-post method used to identify the best Pareto-optimal solution was the technique for order performance by similarity to ideal solution (TOPSIS) [43]. The decision matrix A for the present problem composed of values of criteria or objectives, and the weighting matrix X , which in this case, is represented by the wind power and PV fractions found in each optimum Pareto solution, can be illustrated by Eq. (12) and Eq.13, respectively:

$$A = \begin{bmatrix} y_{11} & \cdots & y_{1n} \\ \cdots & \cdots & \cdots \\ y_{m1} & \cdots & y_{mn} \end{bmatrix} \tag{12}$$

$$X = [x_1, x_2, \ldots, x_n] \tag{13}$$

The evaluation criteria can be classified into two types: benefit and cost. Benefit indicates that the direction of optimization is desired (A^+), whereas for criterion, cost is the inverse (A^-). As the data of matrix A have different origins, the matrix must be normalized to transform it into a dimensionless matrix for the comparison of different objectives of the problem. Matrix A is normalized as follows:

$$y_{ij}^* = \frac{y_{ij}}{max(\bar{y})} \tag{14}$$

Thus, the normalized matrix A_n, representing the performance of the alternatives, can be illustrated by , with $i = 1,\ldots,m$ and $j = 1,\ldots,n$.

The calculation of the best Pareto-optimal solution from TOPSIS is done through the following steps.

1) Calculation of A^+ and A^- as follows:

$$A^+ = (y_1^{*+}, y_2^{*+}, \ldots, y_m^{*+}) \tag{15}$$

$$A^- = (y_1^{*-}, y_2^{*-}, \ldots, y_m^{*-}) \tag{16}$$

where

$$y_j^{*+} = (\max_i y_{ij}^*, j \in J_1; \min_i y_{ij}^*, j \in J_2) \quad (17)$$

$$y_j^{*-} = (\min_i y_{ij}^*, j \in J_1; \max_i y_{ij}^*, j \in J_2) \quad (18)$$

where J_1 and J_2 are benefit and cost criteria.

2) Calculation of Euclidean distance between A_i and A^+ and A_i and A^-:

$$d^+ = \sqrt{\sum_{j=1}^{n} x_j (d_{ij}^+)^2} \quad (19)$$

$$d^- = \sqrt{\sum_{j=1}^{n} x_j (d_{ij}^-)^2} \quad (20)$$

where $d_{ij}^+ = y_j^{*+} - y_{ij}$, with $i = 1,\ldots, m$ and $d_{ij}^- = y_j^{*-} - y_{ij}$, with $i = 1,\ldots, m$.

3) Calculation of relative proximity C^* for each alternative A_i in relation to the ideal solution of A^+:

$$C^* = \frac{d^-}{(d^+ + d^-)} \quad (21)$$

4) Choose Pareto-optimal solution with the largest C*, which is the closest to the optimal positive solution.

Measurements of variables analyzed in farm

Herein, we present the calculations of the objectives considered for the optimal W-PV farm share: AEP, *sd*AEP, P_{min}, and area. The share of MDOE was based on the simplex lattice, with two components (wind and PV) and at 10°, with the inclusion of axial points and a center point, totaling fourteen scenarios to calculate each variable, as listed in Table 1.

Wind and photovoltaic power

The procedures to calculate the AEP of the hybrid farm are presented here. The *sd*AEP of the farm is also used in the same calculation but is obtained by a stochastic process performed by the Monte Carlo simulation (MCS). Five thousand simulations were performed, varying the monthly wind speeds and monthly hours of sunlight in the Weibull probability distributions.

The MCS processed numerous different models, using random values from predetermined probability distributions for the uncertain parameters [44–45]. Several samplings of the parameter inputs were performed by the execution of simulation rounds. Eq. (22) describes the stochastic process to calculate the AEP expected by the MCS, as a function of monthly wind speeds and monthly hours of insolation.

Table 1
Simplex *lattice* share for mixture design of experiment.

x_1 Wind power (MW)	x_2 Photo voltaic power (MW)
30.0	0.0
27.0	3.0
24.0	6.0
22.5	7.5
21.0	9.0
18.0	12.0
15.0	15.0
12.0	18.0
9.0	21.0
7.5	22.5
6.0	24.0
3.0	27.0
0.0	0.0

$$AEP(v_1. ..v_n; h_1. ..h_n) = \int_0^{+\infty} fdp(\widetilde{AWEP}) d\widetilde{AWEP} + \int_0^{+\infty} fdp(\widetilde{APVEP}) d\widetilde{APVEP} \quad (22)$$

where *AEP* is the annual electricity production, *AWEP* is the annual wind electricity production, *APVEP* is the annual PV electricity production, v_i is the mean wind speed in month *i*, h_i is the mean insolation hour in month *i*, and *fdp* is the function density probability.

When performing the AEP simulations using the Crystal Ball® software, the probability distribution with the predicted values and statistical data for the series of results calculated by the simulation are obtained. One of the calculated parameters is *sd*AEP, which has been considered in the analysis.

To estimate AWEP, the electricity was calculated with 8,760 h of recovery, discounting an approximate 7% loss of electricity [45]. Power curves for wind turbines from the manufacturer Enercon were also considered, with powers of 2 MW, 2.3 MW, 3 MW, and 4.2 MW [46], and values of $\eta = 0.98$ and $\rho = 1.225$ kg/m^2 were used [24]. The wind speed data to estimate the wind power were collected from the SWERA base [47] for Caetite, and similar to Aquila et al. [28], the wind speed data were corrected for turbine heights. A mix of wind turbines for each scenario was simulated to achieve best the AWEP.

In the stochastic estimate of wind electricity, uncertainty was incorporated in the average monthly wind speed. The two-parameter Weibull functions are the most appropriate to fit the wind speed [48] and were inserted with specific parameters for 12 months of the year for the lifetime of the W-PV farm of 240 months.

To estimate the parameters of the Weibull distribution, the shape factor (*k*) of 2.00 was used for each month for the wind farms in the state of Bahia [49], and the scale factor (*c*) was calculated using Eq. (23) [50].

$$c = \frac{v}{\Gamma\left(1 + \frac{1}{k}\right)} \quad (23)$$

where *k* is the shape factor (dimensionless) and *c* is the scale factor (m/s).

Table 2 lists the average wind speeds used to estimate the AWEP and the parameters of the Weibull distribution. Thus, MCSs were performed, incorporating uncertainty into the wind behavior.

PV cell data from Yingli Solar [51] were used to estimate the annual average PV electricity production (APVEP). In the scenario with 100% PV power, 100,000 PV cells were considered, and for other scenarios, a proportional percentage of PV power was assumed.

In the stochastic calculation of part of the APVEP, uncertainties were attributed to average sunshine hours for each month of the year, compatible with monthly seasonality. However, to estimate the parameters of the Weibull distributions, sunshine hours for each month between 1994 and 2017 were collected from the INMET base [52].

Using the data series of hours of insolation, it was verified that the Weibull distribution represented a good fit for the data, and with these

Table 2
Average monthly wind speeds and Weibull parameters.

Mounth	v_i	*c*	*k*
Jan	7.36	5.56	2.00
Feb	7.76	5.86	2.00
Mar	7.25	5.47	2.00
Apr	7.81	5.90	2.00
May	7.99	6.04	2.00
Jun	7.70	5.82	2.00
Jul	8.46	6.39	2.00
Aug	7.49	5.66	2.00
Sep	7.45	5.63	2.00
Oct	8.07	6.09	2.00
Nov	8.07	6.09	2.00
Dec	7.90	5.97	2.00

Table 3
Mean hours of insolation and Weibull parameters.

Month	h_i	C	k
Jan	7.70	8.36	5.40
Feb	7.91	8.39	8.19
Mar	7.08	7.56	7.14
Apr	7.22	7.69	7.21
May	7.06	7.40	10.88
Jun	7.22	7.50	13.08
Jul	7.63	7.92	13.94
Aug	8.55	8.22	18.76
Sep	8.64	8.98	11.13
Oct	8.14	8.74	6.94
Nov	6.08	6.68	4.55
Dec	6.36	6.99	4.03

parameters, each distribution was estimated using Crystal Ball® software. Table 3 lists the average hours of insolation and Weibull parameters for each month of the year.

Minimum price

The net present value (NPV) can be used to determine the P_{min} at which the electricity must be sold to reach the minimum return on investment. The NPV is calculated using a discounted cash flow with a rate calculated by the weighted average capital cost (WACC) approach used in several studies related to RET systems [53–56]. The NPV calculation is illustrated as follows:

$$NPV = \frac{\sum_{y=1}^{Y} CFy}{(1+r)^y} - C_0 \tag{24}$$

where Y is the lifetime of the investment, CF_y is the net cash flow in period y, y is the period analyzed, C_0 is the initial investment, and r is the discount rate.

$$WACC = \frac{S}{S+D}k_S + \frac{D}{S+D}k_D \times (1-T) \tag{25}$$

where S is the amount of equity used to finance the investment, k_S is the equity rate of return, D is the amount of debt used to finance the investment, k_D is the cost of the loaned capital, and T is the income tax rate (%).

The capital asset pricing model (CAPM) was applied to calculate k_S, with a country risk premium, estimated as 2.62%, added [53]. The k_S in the CAPM is given as follows:

$$k_S = R + \beta(R_m - R) + R_b \tag{26}$$

where R is the risk-free rate of return (%), R_m is the average return on equity from the stock market (%), β is the factor measuring the risk level, and R_b is the country risk premium.

Eq. (27) was used for the cost of the loaned capital (k_D) [57–58], where R_c is the credit risk.

$$k_D = R_f + R_c + R_b \tag{27}$$

The structure for calculating the free cash flow of the W-PV farm for each period is shown in Table 4.

Table 4
Structure of cash flow for wind-photovoltaic farm in presumed profit.

(+) Gross Sale balance
(−) Taxes proportional to balance
(=) Liquid balance
(−) O&M costs
(=) Results before tax over legal entity/social contribution over liquid profit
(−) Tax over legal entity/social contribution over liquid profit
(−) Investment
(=) Cash flow

Gross sales revenue is equal the product of the amount of electricity produced and the P_{min} to obtain an NPV with an estimated physical guarantee. Taxes collected on the revenue are PIS and Cofins, with rates corresponding to the presumed profit of the investment. Operating expenses refer to the sector charges (ANEEL rate, ONS rate, CCEE rate, and rate of use of the distribution system), lease, operating and maintenance cost (O&M), and insurance expenses.

For the investment values of the wind and PV fractions of the farm, a baseline was calculated using the results of auctions in 2014 and 2015, which include the latest disclosed investment values.

In Table A1 (in appendix), the premises, their respective values, and the source of data are listed.

Occupied area

By minimizing the area used by the plant, the local territory can be used for other productive activities. In some regions or countries, the space available for the deployment of W-PV plants will exhausted quickly. If part of the area that could be occupied by a plant is preserved, the project investor may also reserve an option for future expansion when it is economically favorable and learning gains related to the operation of the system have been achieved. A measure of productivity to be considered is the energy density, which indicates the capacity of the system to produce maximum energy per occupied space.

Based on the occupied area in km^2 per installed GW, the area occupied by a hybrid farm with 0.03 GW can be inferred as 297 km^2 and 18.9 km^2 for wind and PV, respectively [36]. Therefore, the area occupied by a W-PV farm with different compositions can be calculated as follows:

$$297x_1 + 18.9x_2 \tag{28}$$

Results

The optimum parameters of W-PV farms, using the method that we have named NBI-EFA-SNR as the fundamental tool for the optimization process, can be determined from the 7 steps that are illustrated in Fig. 2.

Step 1 is represented by the scenarios from MDOE shown in Table 1. Then, in *Step 2*, the values of AEP, *sd*AEP, P_{min}, and area are estimated for each scenario presented in Table 1. Among the variables considered in the analysis in this study, it is desired to maximize AEP and minimize *sd*AEP, P_{min}, and area. Therefore, in *Step 3*, the sense of optimization for the AEP variables will be inverted by means of Eq. (3) ("smaller-the-better"). With the direction of the inverted AEP variable, the objective of the optimization problem will be the minimization of the factor functions. In Table 5, all the values of all the variables calculated in *Step 2*, other than the SNR of the AEP variable calculated in *Step 3*, are illustrated.

Subsequently, a correlation analysis is performed between the SNR-AEP, *sd*AEP, P_{min}, and area responses. P-value < 0.05 confirms the existence of a correlation between all response variables, as shown in Table 6.

After confirming the existence of the correlations, in *Step 4* an EFA is performed. The original correlation matriz (Σ) related to the analyzed data is illustrated in Eq. (29). The orthogonal model is applied, with loadings estimated from the analysis of the main components, and an equimax rotation is utilized to rotate the loadings.

$$\sum = \begin{bmatrix} 1.000 & -0.970 & -0.977 & 0.976 \\ -0.970 & 1.000 & 0.991 & -0.954 \\ -0.978 & 0.991 & 1.000 & -0.983 \\ 0.976 & -0.954 & -0.983 & 1.000 \end{bmatrix} \tag{29}$$

An EFA with the rotation from equimax explains that from two factors, we obtain the information of four variables analyzed in the problem, as listed in Table 7 and displayed in the scree plot in Fig. 3. Therefore, the optimization of a hybrid farm that would initially be

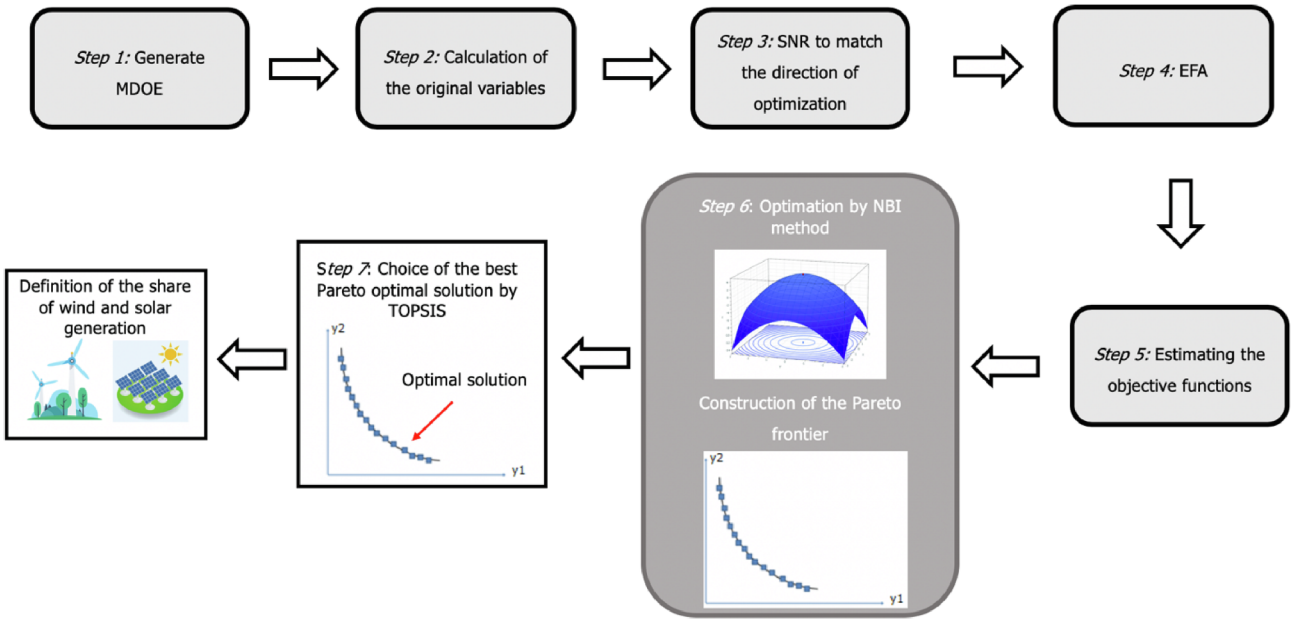

Fig. 2. Steps for optimal share of wind-photovoltaic farm.

Table 5
Simplex *lattice* share for mixture design of experiment.

x_1 wind power (MW)	x_2 Photovoltaic power (MW)	AEP (GWh)	SNR-AEP	*sd*AEP	P_{min} (R $/MWh)	Area (km^2)
30.0	0.0	109.89	−40.82	4.44	109.72	297.00
27.0	3.0	102.29	−40.20	3.67	117.97	269.19
24.0	6.0	96.55	−39.70	3.54	127.47	241.38
22.5	7.5	79.62	−38.02	2.42	154.10	227.48
21.0	9.0	89.70	−39.06	3.06	138.25	213.57
18.0	12.0	83.59	−38.44	2.62	150.57	185.76
15.0	15.0	78.98	−37.95	2.14	164.79	157.95
12.0	18.0	72.88	−37.25	1.77	181.39	130.14
9.0	21.0	66.51	−36.46	1.33	201.01	102.33
7.5	22.5	57.48	−35.19	2.42	236.37	88.43
6.0	24.0	60.36	−35.62	0.98	224.57	74.52
3.0	27.0	54.18	−34.68	0.61	201.01	46.71
0.0	30.0	48.20	−33.66	0.52	289.42	18.90

Table 6
Results of correlation analysis.

	Area	P_{min}	AEP
P_{min}	−0.97p-value (0.00)	–	
AEP	−0.978p-value (0.00)	0.991p-value (0.00)	–
*sd*AEP	0.976p-value (0.00)	−0.954p-value (0.00)	− 0.983p-value (0.00)

solved using four objective functions can now be solved using two functions.

The scree plot illustrated in Fig. 3 characterizes that two factors are sufficient to explain the information represented by the four variables to be optimized for the configuration of the W-PV farm.

The biplot shown in Fig. 4 complements the loading plot information (Fig. 3). In this case, it is possible to observe in detail how the first two factors concentrate the information on the four variables analyzed in the problem.

As Table 7 shows, the first factor explains 54% of the variance of the set, and the second factor explains 46%. As the loading plot of Fig. 5 indicates, for the first factor, the AEP and P_{min} variables have a negative loading, whereas for sdAEP and area, the loading is positive. The situation is reversed for the second factor, with a positive loading for AEP and P_{min} and negative loading for sdAEP and area.

Table 7
Exploratory factor analysis results.

	First Factor	Second Factor
Eigenvalue	3.95	0.025
Proportion	54%	46%
Accumulated	54%	100%
Eigenvectors	**First Factor**	**Second Factor**
Area	−0.50	−0.36
P_{min}	0.499	0.36
AEP	0.498	−0.84
*sd*AEP	−0.50	−0.12

Scores for the first and second factor (F_1 and F_2) were also obtained for each scenario generated from MDOE and are listed in Table 8. In *Step 5*, the values of F1 and F2 are used to performed quadratic regressions that provide the objective functions to be used in the NL-MO with the NBI method.

The quadratic regression used to obtain the objective functions of F_1 and F_2 includes two additional terms, which contributed to the increase in the adjusted R^2 (R^2_{adj}) of the equations. The quadratic regressions were also performed to obtain the AEP, *sd*AEP, and P_{min} functions. Table 9 lists the functions for F_1 and F_2, and Table 10 contains the functions of AEP, *sd*AEP, P_{min}, and area after the optimal percentage of wind power and PV power is determined.

In *Step 6*, functions F1 and F2 are optimized using the NBI method. First, the payoff matrix was elaborated, as indicated in Eq. (11), and then the multi-objective problem was solved using the NBI routine illustrated in Eq. (10). In Eq. (35), the formulation for the multi-objective problem related to the configuration of W-PV farms was described mathematically.

$$\begin{aligned} Min \quad & F_1 = -2.23x_1 - 0.32x_2 + 7.25x_1x_2 - 2.38x_1x_2(x_1 - x_2) \\ & + 4.64x_1x_2(x_1 - x_2)^2 \\ Min \quad & F_2 = -0.02x_1 - 2.62x_2 + 8.06x_1x_2 - 3.08x_1x_2(x_1 - x_2) \\ & + 2.12x_1x_2(x_1 - x_2)^2 \\ & s.\,t.: \quad \sum_{i=1}^{n} w_i = 1 \\ & 0 \leqslant w_i \leqslant 1 \end{aligned} \tag{35}$$

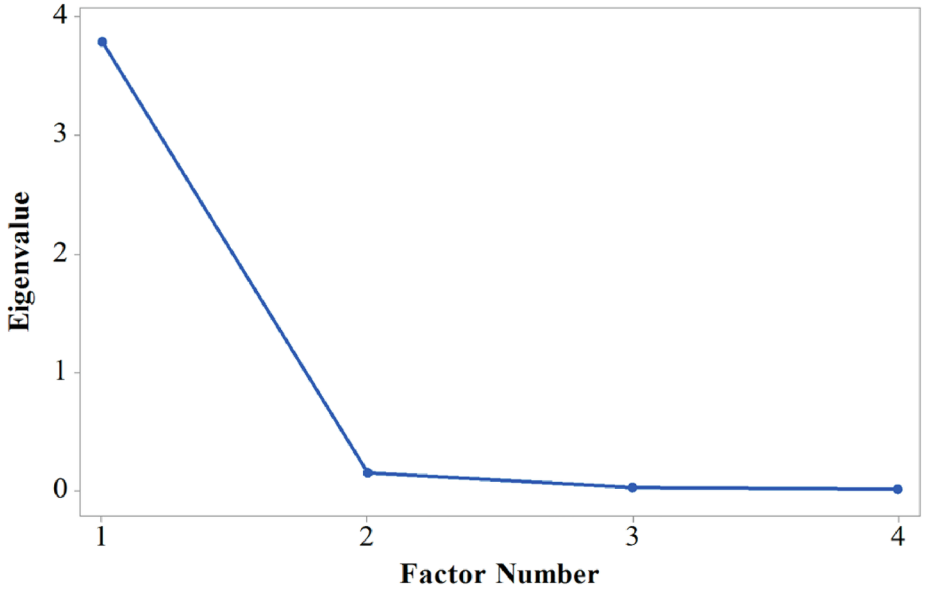

Fig. 3. Scree Plot.

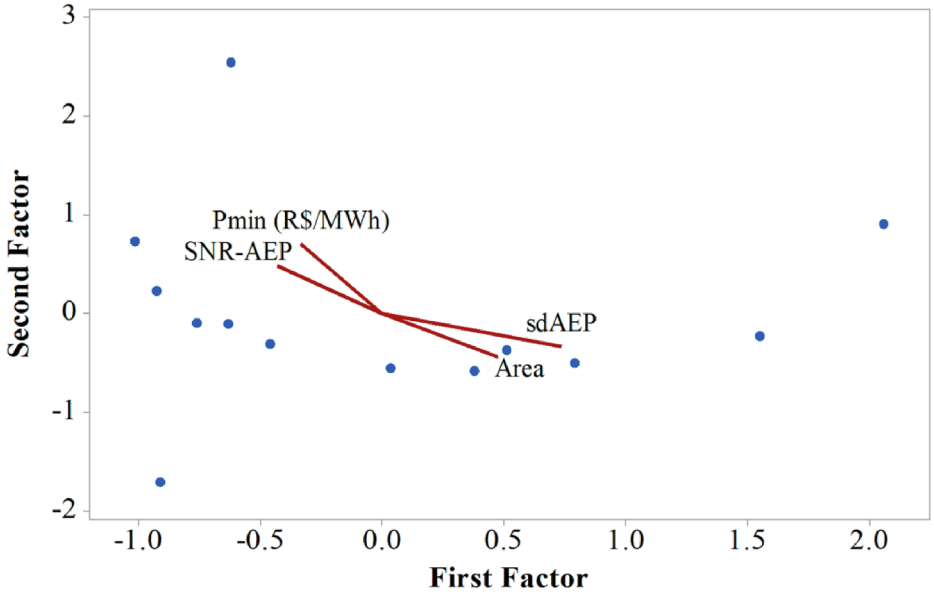

Fig. 4. Biplot for two factors.

For the NBI results, a Pareto frontier was designed in an equally distributed form, with the function weights varying by 0.05 in each round of optimization, resulting in 20 Pareto solutions. After the design of the Pareto frontier, best Pareto-optimal solution was selected from TOPSIS, and the solution with highest C* value was considered to be the best Pareto-optimal solution.

The 20 solutions determined by the Pareto frontier are illustrated in Table 11, and the best Pareto-optimal solution is highlighted in the Pareto frontier of Fig. 6.

In Table 11 and the Pareto frontier in Fig. 6, the ideal composition for W-PV in Caetité is 41% wind power and 59% PV power. That figure corresponds to approximately 12.3 MW of wind power and 17.7 MW of PV power for a 30 MW farm. In an existing farm, the composition is 82% wind power and 18% PV power. This result reinforces that the use of models that consider numerous objectives relevant to the electric sector, especially those related to maximization of well-being, can provide more favorable decisions for all stakeholders, without causing financial damage to the investor.

According to Fig. 6, using the proposed approach for planning a W-PV farm, it was possible to build the Pareto border two-dimensionally, with the solutions of the problem presented more visibly than using the multi-objective method with the original four responses. For the present problem, for example, a traditional approach would be impossible to graphically represent the problem with four dimensions. In addition, the computational cost would be much higher, and the problem resolution would be greater with more objectives to be optimized.

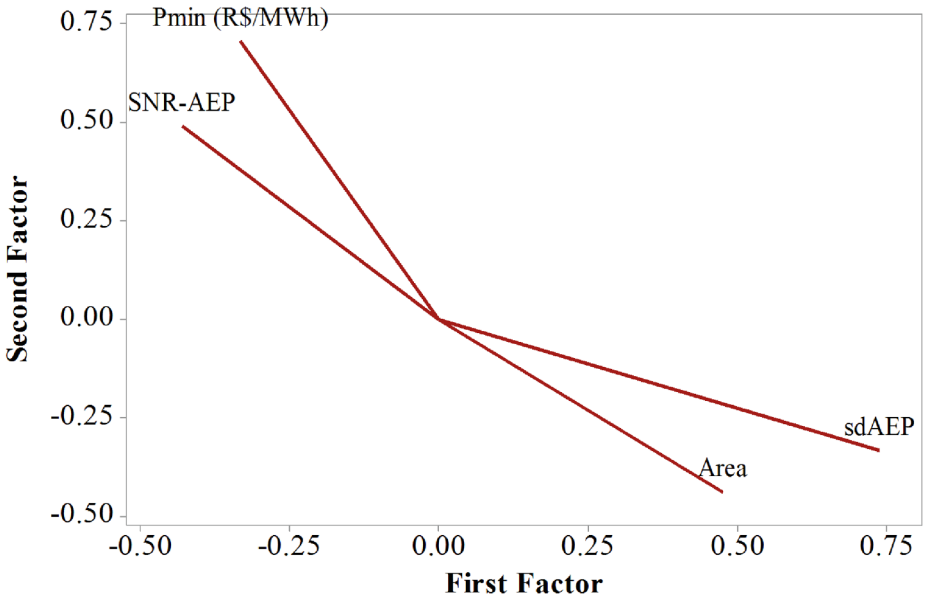

Fig. 5. Loading Plot.

Table 8
Factor score for each scenario.

x_1 wind power (MW)	x_2 Photovoltaic power (MW)	F_1	F_2
30.0	0.0	−2.30	−0.13
27.0	3.0	−1.06	0.64
24.0	6.0	−0.98	0.44
22.5	7.5	−0.11	0.50
21.0	9.0	−0.35	0.65
18.0	12.0	0.14	0.74
15.0	15.0	0.67	0.86
12.0	18.0	0.88	0.63
9.0	21.0	1.09	0.36
7.5	22.5	0.69	−0.68
6.0	24.0	0.99	−0.24
3.0	27.0	0.69	−1.09
0.0	30.0	−0.35	−2.68

Another fundamental question is that the traditional methods of multi-objective optimization do not address the question of the correlation between the answers, which can bring serious distortions to the resolution of the problem and induce Pareto-optimal responses that would be impossible to achieve in reality.

Finally, the approximate values of AEP, *sd*AEP, P_{min}, and area were estimated using Eq. 32, 33, and 34 for W-PV with the optimum composition of 41% wind power and 59% PV power. The estimated results are in Table 12.

The proposed approach had reached the objective of finding an optimal configuration for W-PV farms, while optimizing multiple correlated responses. Thus, the approach could be a possible mechanism to support the bidding process for W-PV farms and guide the criteria for investors to define the ideal share of each source. Finally, outputs and restrictions can be added to meet the context of the electricity sector and the marketing schemes for investors.

Conclusions

This study aimed to propose a new approach to determine the optimum parameters of hybrid farms, using normal boundary intersection (NBI), exploratory factor analysis (EFA) and Taguchi signal-to-noise ratio (SNR), characterized NBI-EFA-SNR method. This method presents greater flexibility in the modeling process, which can be applied to several types of electricity systems using various sources.

In this study, the model was applied to reach an optimal share for a wind-photovoltaic (W-PV) farm in which variables that impact environmental issues are considered, such as area occupied by the farm and electricity security, while also seeking the maximum production with the lowest possible financial risk to investors and the final consumer. Furthermore, this method has been shown to guarantee environmental and electricity security objectives, without compromising the profitability of the investment.

The results of EFA and scree plot reveal that from the eigenvalues of the experimental matrix results, two factors are sufficient to explain 100% of the information related to the four correlated outputs to be optimized. Thus, it was possible to develop the optimization problem with only two objective functions and find the optimal share of 41% wind and 59% PV.

The optimal results achieved are AEP = 72.17 GWh, sdAEP = 1.74, P_{min} = 182.95 R$/MWh, and area = 132.92 km^2. Because of the conflicting behavior of the objectives, the optimization process implies that improving one objective impairs the others. Thus, a higher AEP

Table 9
F_1 and F_2 functions for optimization.

Variable	R^2_{adj}	y_1
F_1	94.70%	$-2.23x_1 - 0.32x_2 + 7.25x_1x_2 - 2.38x_1x_2(x_1\text{-}x_2) + 4.64\, x_1x_2(x_1\text{-}x_2)^2$ (30)
F_2	91.77%	$-0.02x_1 - 2.62x_2 + 8.06_1x_2 - 3.08x_1x_2(x_1\text{-}x_2) + 2.12\, x_1x_2(x_1\text{-}x_2)^2$ (31)

Table 10
AEP, *sd*AEP, P_{min} and area functions.

Variable	R^2_{adj}	y_1
AEP	95.09%	$-40.93x_1 - 33.72x_2 - 1.91x_1x_2 + 2.30x_1x_2(x_1\text{-}x_2) + 5.15\,x_1x_2(x_1\text{-}x_2)^2$ (32)
*sd*AEP	95.26%	$4.45x_1 + 0.55x_2 - 1.33x_1x_2 + 0.07x_1x_2(x_1\text{-}x_2) - 4.58x_1x_2(x_1\text{-}x_2)^2$ (33)
P_{min}	96.89%	$108.03x_1 + 287.36x_2 - 123.76x_1x_2 + 50.33x_1x_2(x_1\text{-}x_2) + 72.10x_1x_2\,(x_1\text{-}x_2)^2$ (34)
Area	100%	Eq.32

Table 11
Optimization results.

x_1	x_2	y_1	y_2	C*
100%	0%	−2.23	−0.03	0.690
92%	8%	−1.43	0.28	0.568
87%	13%	−1.09	0.42	0.542
82%	18%	−0.75	0.54	0.512
76%	24%	−0.43	0.64	0.504
69%	31%	−0.15	0.71	0.560
63%	37%	0.11	0.74	0.660
57%	43%	0.32	0.74	0.754
51%	49%	0.51	0.70	0.828
46%	54%	0.67	0.63	0.880
41%	59%	0.80	0.54	**0.901**
36%	64%	0.90	0.41	0.872
32%	68%	0.97	0.26	0.802
28%	72%	1.00	0.06	0.707
23%	77%	0.99	−0.17	0.630
19%	81%	0.93	−0.46	0.627
15%	85%	0.81	−0.83	0.660
10%	90%	0.58	−1.30	0.693
5%	95%	0.17	−1.95	0.719
0%	100%	−0.32	−2.62	0.734
0%	100%	−0.32	−2.62	0.734

and smaller P_{min} produce a larger sdAEP and area.

Notably, the primary contribution of the method is to provide a more flexible criterion to define the share of hybrid farms, especially W-PV, in the bidding process. In the developed model, the application of EFA and SNR to assist in the design of the method is a new approach. The model is applicable to any electric system regardless of its characteristics and allows for the inclusion of several variables with a low computational cost. The method was able to indicate an optimal solution using information related to wind and PV resources of the region and the technical characteristics of the farm.

Table 12
Results estimated for wind-photovoltaic in optimum share.

Variable	Results
AEP (GWh)	72.17
*sd*AEP (GWh)	1.74
P_{min} (R$/MWh)	182.95
Area (km^2)	132,92

The proposed approach can be extended to more complex cases, involving restrictions related to system operations in addition to other technical restrictions. Moreover, other sources of renewable energy can be applied to the system by changing the inputs and the objectives to be optimized according to the planning requirements of each system. For future research, the approach of this study can be applied to systems with energy storage, other types of hybrid RES plants (wind + hydro, PV + hydro, biomass + coal, and others), and systems that use more than two energy sources, such as RES sources.

CRediT authorship contribution statement

Giancarlo Aquila: Conceptualization, Methodology, Formal analysis, Investigation, Software, Writing - original draft, Writing - review & editing, Visualization. **Anderson Rodrigo de Queiroz:** Conceptualization, Methodology, Formal analysis, Investigation, Writing - original draft, Writing - review & editing, Visualization. **Paulo Rotela Junior:** Formal analysis, Investigation, Writing - original draft, Writing - review & editing, Visualization. **Luiz Célio Souza Rocha:** Conceptualization, Methodology, Formal analysis, Investigation, Writing - original draft, Visualization. **Edson de Oliveira Pamplona:** Resources, Data curation, Supervision. **Pedro Paulo Balestrassi:**

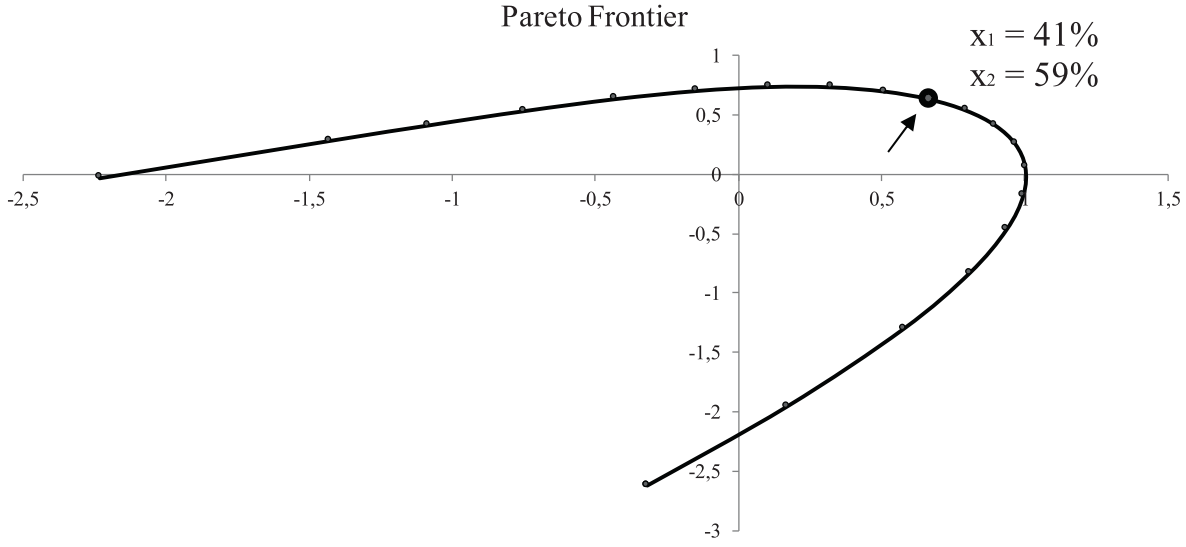

Fig. 6. Pareto frontier.

Resources, Data curation, Supervision, Funding acquisition, Supervision.

Declaration of Competing Interest

The authors declare that they have no known competing financial interests or personal relationships that could have appeared to influence the work reported in this paper.

Acknowledgments

We thank the CNPq - National Council for Scientific and Technological Development (Brazil): CNPq Fellow - Brazil (155507 / 2018-4). Also, the authors would like to thank Capes and Fapemig.

Appendix

Table A1
Data used to calculate $P_{min.}$

Parameters	Value	Reference
Investment (wind fraction)	R$ 3,918,623.32 per MW installed	[55]
Investment (Photovoltaic fraction)	R$ 4,795,304.68 per MW installed	[55]
Planning horizon	20 years	[45]
Lease	R$ 68.73/ km^2	[45]
O&M Costs (wind fraction)	2% of the investment	[45]
O&M Costs (Photovoltaic fraction)	0.5% of the investment	[59]
Transmission system usage fee	R$ 4.85/ kW installed	[45]
CCEE Tax	R$ 0.07 per MWh of assured energy	[45]
ONS Tax	R$ 0.47 per kW installed	[45]
ANEEL Tax	R$ 2.56 per kW installed	[45]
Insurance Expenses	0.3% of the investment	[56]
Others taxes	3% (PIS) and 0.65% (Cofins)	[45]
Tax over legal entity	25% over 8% of gross revenue	[45]
Social contribution over the liquid profit	9% over 12% of gross revenue	[45]
D	63.55%	[60]
E	35.45%	[60]
R_f	2.73%	[58] (29.09.16–29.09.2017)
R_m	7.56%	[60]
R_b	2.62%	[60]
β	1.14	[57]
k_e	13.97%	Eq.17
k_d	8.72%	Eq.18
$_{Rc}$	3.37%	[60]
τ	34%	[45]
WACC (discount rate)	**6.19%**	Eq. (16)

Appendix A. Supplementary data

Supplementary data to this article can be found online at https://doi.org/10.1016/j.seta.2020.100754.

References

[1] Hilee E, Althammer W, Diedrich H. Environmental regulation and innovation in renewable energy technologies: Does the policy instrument matter? Technol Forecast Soc Change 2020;153:119921.
[2] Kumar S. Assessment of renewables for energy security and carbon mitigation in Southeast Asia: the case of Indonesia and Thailand. Appl Energy 2016;163:63–70.
[3] Shezan SKA, Julai S, Kibria MA, Saidur R, Chong WT, Akikur RK. Performance analysis of an off-grid wind-PV (photovoltaic)-diesel-battery hybrid energy system feasible for remote areas. J Clean Product 2016;125:121–32.
[4] Davis W, Martin M. Optimal year-round operation for methane production from CO2 and water using wind and/or solar energy. J of Clean Product 2014;80:252–61.
[5] Abdomouleh Z, Ram Alammari, Gastli A. Review of policies encouraging energy integration & best practices. Renew Sustain Energy Rev 2015;45:246–62.
[6] Balsalobre-Lorente D, Shahibaz M, Roubaud D, Farhani S. How economic growth, renewable electricity and natural resources contribute to CO2 emissions? Energy Policy 2018;113:356–67.
[7] Lee M, Hong T, Kho C. An economic impact analysis of state solar incentives for improving financial performance of residential solar photovoltaic systems in the United States. Renew Sust Energ Rev 2016;58:590–607.
[8] Mignon I, Bergek A. Investments in renewable electricity production: The importance of policy revisited. Renew Energy 2016;88:307–16.
[9] Abolhosseini S, Heshmati A. The main support mechanisms to finance renewable energy development. Renew Sustain Energy Rev 2014;40:876–85.
[10] Stoke LC. The politics of renewable energy policies: The case of feed-in tariffs in Ontario. Canada. Energy Policy 2013;56:490–500.
[11] Shum KL, Watanbe C. Network externality perspective of feed-in tariffs (FIT) instruments – Some observations and suggestions. Energy Policy 2013;38:3266–9.
[12] Nalan ÇB, Murat Ö, Nuri Ö. Renewable energy market conditions and barriers in Turkey. Renew Sust Energ Rev 2009;13:1428–36.
[13] Romano AA, Scandurra G, Carfora A, Fodor M. Renewable investments: The impact of green policies in developing and developed countries. Renew Sust Energ Rev 2017;68:738–47.
[14] Oree V, Hassen SZS, Fleming PJ. Generation expansion planning optimisation with renewable energy integration: A review. Renew Sust Energ Rev 2017;69:790–803.
[15] Park JB, Park YM, Won JR, Lee KY. An improved genetic algorithm for generation expansion planning. IEEE Trans Power Syst 2000;15:916–22.
[16] Kannan S, Slochanal SMR, Padhy NP. Application and comparison of metaheuristic techniques to generation expansion planning problem. IEEE Trans Power Syst 2005;20:466–75.
[17] Sirikum J, Techanitisawad A, Kachitivichyanukul V. New efficient GA-Benders' decomposition method: for power generation expansion planning with emission controls. IEEE Trans Power Syst 2007;22:1092–100.
[18] Mavrotas G, Diakoulaki D, Papayannakis L. An energy planning approach based on mixed 0 ± 1 Multiple Objective Linear Programming. Int T Oper Res 1999;6:231–44.
[19] Antunes CH, Martins AG, Brito IS. A multiple objective mixed integer linear programming model for power generation expansion planning. Energy 2004;29:613–27.
[20] Aghaei J, Akbari MA, Roosta A, Gitizadeh M, Niknam T. Integrated renewable–conventional generation expansion planning using multiobjective framework. IET Gener Transm Dis 2012;6:773–84.
[21] Vahidinasab V, Jadid S. Normal boundary intersection method for suppliers'

strategic bidding in electricity markets: An environmental/economic approach. Energ Convers Manage 2010;51:1111–9.
[22] Aghaei J, Akbari MA, Roosta A, Baharvandi A. Multiobjective generation expansion planning considering power system adequacy. Electr Pow Syst Res 2013;102:8–19.
[23] Ahmadi A, Kaymanesh A, Siano P, Janghorbani M, Nezhad AE, Sarno D. Evaluating the effectiveness of normal boundary intersection methodfor short-term environmental/economic hydrothermalself-scheduling. Electr Pow Syst Res 2015;123:192–204.
[24] Izadbakhish M, Gandomkar M, Rezvani A, Ahmadi A. Short-term resource scheduling of a renewable energy based micro grid. Renew Energy 2015;75:598–606.
[25] Luz T, Moura P, Almeida A. Multi-objective power generation expansion planning with high penetration of renewables. Renew Sust Energ Rev 2017;81:2637–43.
[26] Fonseca MN, Pamplona EO, Queiroz AR, Valerio VEM, Aquila G, Silva SR. Multi-objective optimization applied for designing hybrid power generation systems in isolated networks. Sol Energy 2018;161:207–19.
[27] Roberts JJ, Cassula AM, Silveira JL, Bortoni EC, Mendiburu AZ. Robust multi-objective optimization of a renewable based hybrid power system. Appl Energy 2018;223:52–68.
[28] Aquila G, Rocha LCS, Pamplona EO, Queiroz AR, Rotela Junior P, Balestrassi PP, et al. Proposed method for contracting of wind-photovoltaic connected projects to the Brazilian electric system using multiobjective programming. Renew Sust Energ Rev 2018;97:377–89.
[29] Rao SS. Engineering optimization: theory and practice. 4th ed. New Jersey: John Wiley & Sons; 2009. p. 813.
[30] Nocedal J, Wright SJ. Numerical optimization. 2nd ed. New York: Springer; 2006. p. 683.
[31] Cornell J. Experiments with mixtures: designs, models, and the analysis of mixture data. 3rd ed. New York: John Wiley & Sons; 2002. p. 649.
[32] Ren G, Wan J, Liu J, Yu D. Spatial and temporal assessments of complementarity for renewable energy resources in China. Energy 2019;177..
[33] Monforti F, Huld T, Bodis K, Vitali L, D'Isidoro M, Lacal-Arantegui R. Assessing complementarity of wind and solar resources for energy production in Italy. A Monte Carlo approach. Renew. Energy 2014;63..
[34] Hoicka CE, Rowlands IH. Solar and wind resource complementarity: advancing options for renewable electricity integration in Ontario, Canada. Renew. Energy 2011;36:1.
[35] Fadigas EAFA. Wind Energy (in portuguese), Manole; 2011, p. 285.
[36] Ramanathan R. Comparative Risk Assessment of energy supply technologies: A Data Envelopment Analysis approach. Energy 2001;26:197–203.
[37] Montgomery DC. Design and Analysis of Experiments. 7th ed. New York: John Wiley & Sons; 2009. p. 665.
[38] Timm NH. Applied Multivariate Analysis. New York: Springer texts in statistics; 2002. p. 515–30.
[39] Johnson RA, Wichern DW. Applied multivariate statistical analysis. 5th ed. New Jersey: Pretience-Hall Inc.; 2002.
[40] Rencher A. Methods of Multivariate Analysis. 2nd ed. New Jersey: John Wiley & Sons; 2002.
[41] Darton RA. Rotation in Factor Analysis. J Royal Stat Soc Series D (The Statistician) 1980;29:167–94.
[42] Das I, Dennis JE. Normal-boundary intersection: A new method for generating the Pareto surface in nonlinear multicriteria optimization problems. SIAM J Optimiz 1998;8:631–57.
[43] Hwang CL, Yoon KP. Multiple attributes decision making methods and applications. Berlin: Springer-Verlag; 1981. p. 350.
[44] Jiang Y, Nan Z, Yang S. Risk assessment of water quality using Monte Carlo simulation and artificial neural network method. J Environ Manage 2013;122:130–6.
[45] Aquila G, Rotela Junior P, Pamplona EO, Queiroz AR. Wind power feasibility analysis under uncertainty in the Brazilian electricity market. Energy Econ 2017;65:127–36.
[46] Enercon. Product line Enercon; 2016.
[47] SWERA – Solar and Wind Energy Resource Assesment. National Renewable Energy Laboratory (NREL) maps; 2017. https://maps.nrel.gov/swera/#/?aL=0&bL=groad&cE=0&lR=0&mC=40.21244%2C-91.625976&zL=4. (accessed March, 2017).
[48] Celik AN. Energy output estimation for small-scale wind power generators using Weibull-representative wind data. J Wind Eng Ind Aerod 2003;91:693–707.
[49] Nota EPE. Técnica DEA 15/13 - Acompanhamento de Medições Anemométrica – AMA: Caracterização do Recurso Eólico e Resultados Preliminares de sua Aplicação no Sistema Elétrico. 46p. EPE: Rio de Janeiro 2013.
[50] Justus C, Hargraves W, Mikhail A, Graber D. Methods for estimating wind speed frequency distributions. J Appl Meteorol 1978;17:350–3.
[51] Yingli Solar. Série de células YGE72; 2015. http://www.yinglisolar.com/br/products/multicrystalline/yge-72-cell-series/. (acessed July, 2017).
[52] INMET - Instituto Nacional de Meteorologia. BDMEP e Dados Históricos; 2018. < http://www.inmet.gov.br/projetos/rede/pesquisa/ > .
[53] Rocha LC, Aquila G, Rotela Junior P, Paiva AP, Pamplona EO, Balestrassi PP. A stochastic economic viability analysis of residential wind power generation in Brazil. Renew Sust Energ Rev 2018;90:412–419.
[54] Rocha LC, Aquila G, Pamplona E, Paiva AA, Chieregatti BG, Lima JS. Photovoltaic electricity production in Brazil: A stochastic economic viability analysis for small systems in the face of net metering and tax incentives. J Clean Prod 2017;168:1448–62.
[55] CCEE. Câmara de Comercialização de Energia Elétrica – O que fazemos: Leilões; 2017. http://www.ccee.org.br/portal/faces/oquefazemos_menu_lateral/leiloes?_afrLoop=5547777042548#%40%3F_afrLoop%3D5547777042548%26_adf.ctrl-state%3Dp6tr9dqjl_112.
[56] COPEL - Companhia Paranaense de Energia. Manual de avaliação técnico-econômica de empreendimentos eólio-elétricos. Curitiba: LACTEC; 2007. 104p.
[57] Damodaran A. Betas by sector (US); 2017 Available at: http://people.stern.nyu.edu/adamodar/New_Home_Page/datafile/Betas.html (accessed in October, 2017).
[58] U.S Department of Treasury. Daily Treasury Long Term Data; 2017. < https://www.treasury.gov/resource-center/data-chart-center/interest-rates/Pages/TextView.aspx?data=longtermrate > . (accessed in October, 2017).
[59] Waissbein O, Glemarec Y, Bayraktar H, Schmidt TS. Derisking Renewable Energy Investment. A Framework to Support Policymakers in Selecting Public Instruments to Promote Renewable Energy Investment in Developing Countries. United Nations Development Programme, New York; 2013.
[60] ANEEL, 2015b. Despacho n°16, de 15 de janeiro de; 2015.Available at: https://duto.aneel.gov.br/concessionarios/taxafiscalizacao/aplicativo/default.asp?flag=2 (Accessed in: April, 2015).